Development 133, 4607 (2006) doi:10.1242/dev.02692

Small molecule-induced ablation and subsequent regeneration of larval zebrafish melanocytes

Chao-Tsung Yang and Stephen L. Johnson

There was an error published in *Development* **133**, 3563-3573.

The chemical name for MoTP used in this study should be 4-(4-morpholinobutylthio)phenol, rather than (2-morpholinobutyl)-4-thiophenol, which specifies a different chemical structure. The structure for MoTP shown in Fig. 4A remains correct.

The authors apologise to readers for this mistake.

Development 133, 3563-3573 (2006) doi:10.1242/dev.02533

Small molecule-induced ablation and subsequent regeneration of larval zebrafish melanocytes

Chao-Tsung Yang and Stephen L. Johnson*

We developed a method to efficiently ablate a single cell type, the zebrafish melanocyte, and study the mechanisms of its regeneration. We found that a small molecule, (2-morpholinobutyl)-4-thiophenol (MoTP), specifically ablates zebrafish larval melanocytes or melanoblasts, and that this melanocytotoxicity is dependent on tyrosinase activity, which presumably converts MoTP to cytotoxic quinone species. Following melanocyte ablation by MoTP treatment, we demonstrate by BrdU incorporation experiments that regenerated melanocytes are derived from the division of otherwise quiescent melanocyte precursors or stem cells. We further show that larval melanocyte regeneration requires the *kit* receptor tyrosine kinase. Our results suggest that a small number of melanocyte precursors or stem cells unevenly distributed in larvae are drawn upon to reconstitute the larval melanocyte population following melanocyte ablation by MoTP.

KEY WORDS: Melanocyte, Regeneration, Chemical ablation, Stem cell, Cell division

INTRODUCTION

One of the enduring challenges of modern biology is a mechanistic understanding of regeneration. In understanding the many strategies used by organisms for regeneration, two important questions are the role of cell division or growth, and the origin of the cells used to replace the missing tissues. Historically, regeneration studies in systems such as the salamander limb or hydra have revealed two major modes of regeneration, epimorphosis and morphallaxis. The salient mechanistic distinction between them is the role of cell division; epimorphosis involves active cellular proliferation and morphallaxis is achieved through re-patterning of the remaining cells without a role for growth or cell proliferation (Morgan, 1901) (reviewed by Lenhoff and Lenhoff, 1991). More recently, attention has focused on the origins of cells contributing to regeneration, revealing roles for both differentiated and undifferentiated precursors in various modes of regeneration. This distinction, combined with Morgan's original distinction based on growth and cell proliferation, suggests four classifications for regeneration mechanisms subject to cell division and differentiated state of regeneration precursors, as follows. (1) Regeneration via direct cell division from differentiated cells (Fig. 1A). This mechanism is sometimes called compensatory regeneration, exemplified by mammalian liver regeneration (reviewed by Michalopoulos and DeFrances, 1997). (2) Regeneration via cell division from undifferentiated precursors or stem cells (Fig. 1B). This mechanism closely matches the current usage of epimorphosis, and is best exemplified by the stage of limb regeneration following formation of the blastema (Chalkley, 1954; Hay and Fischman, 1961). (3) Regeneration without cell division by transdifferentiation from otherwise differentiated cells, as occurs in hydra following resection (Park et al., 1970; Holstein et al., 1991) (Fig. 1C). (4) A fourth, as yet hypothetical, mode of regeneration is formally suggested by this classification scheme and involves regeneration without cell division from late-stage undifferentiated precursors (Fig. 1D). We note that additional mechanisms, such as dedifferentiation of differentiated cells to form a blastema are also employed in some regenerating systems. Additionally, regeneration schemes may combine some of these mechanisms, either sequentially in the same lineage [for instance, in limb regeneration, dedifferentiation of myofibers to form the blastema is then followed by proliferation and new growth (Kintner and Brockes, 1984)] or use different mechanisms for the different cell types or lineages contributing to regeneration of more complex tissues [for instance, in zebrafish fin regeneration, keratinocytes divide directly (Poleo et al., 2001), whereas melanocytes are thought to be derived from undifferentiated precursors or stem cells (Rawls and Johnson, 2000)].

Another opportunity for understanding regeneration and the underlying mechanisms of regulation comes from the analysis of homeostasis of single cell types in mammals, such as erythrocytes (reviewed by Morrison et al., 1995), epidermis (Jones and Watt, 1993) (reviewed by Fuchs and Raghavan, 2002), and epithelium in the lining of the small intestine (Cheng and Leblond, 1974) (reviewed Potten and Loffler, 1990). For each of these examples, the differentiated cells turn over rapidly and homeostatic mechanisms act on stem cells to generate new cells. This ability to replenish certain single cell types is crucial for maintaining the normal physiology and lifespan in humans. For instance, the deficient replenishment of erythrocytes results in anemia, whereas excessive turnover or misregulation of epidermal cells may cause psoriasis or skin cancer (Weinstein and Frost, 1968). Other human diseases result from deficits in single cell types with less capacity for regeneration, such as pancreatic β cells in autoimmune type I diabetes, or oligodendrocytes in multiple sclerosis (for reviews, see Bach, 1994; Compston and Coles, 2002). An understanding of the mechanisms regulating single cell type regeneration in model systems might therefore be used to develop cures for relevant human diseases.

An attractive cell type for this approach is the zebrafish melanocyte, because it is easily visualized, dispensable for viability in the laboratory, and multiple mutations have been generated that affect different aspects of its development at different stages of the fish life cycle. As in other vertebrates, zebrafish melanocytes are derived from the embryonic neural crest (Raible et al., 1992). Melanocytes first appear at 24 hours postfertilization (hpf), and, by

Department of Genetics, Washington University School of Medicine, 4566 Scott Avenue, Saint Louis, MO 63110, USA.

*Author for correspondence (e-mail: sjohnson@genetics.wustl.edu)

Accepted 12 July 2006

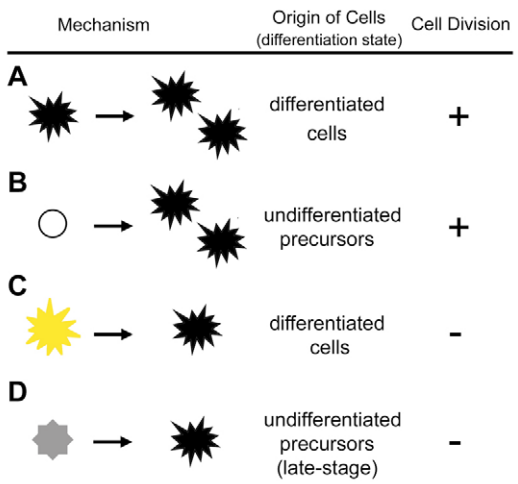

Fig. 1. Four possible modes for melanocyte regeneration distinguished by roles for cell division and the differentiation state of precursors. (**A**) Regeneration involves direct proliferation of pre-existing, differentiated melanocytes and requires no further role for differentiation (compensatory regeneration). (**B**) Regeneration is achieved through the recruitment of quiescent precursors or stem cells to proliferate and differentiate (epimorphosis). (**C**) Regeneration involves transdifferentiation of other differentiated cells without cell division to generate the new melanocytes (morphallaxis). (**D**) Regeneration occurs by direct differentiation of set-aside late-stage undifferentiated precursors (for instance, *dct*$^{+}$ melanoblasts) into melanocytes without cell division. Note that unlike stem cell-based models, regeneration by this last mechanism would tend to exhaust the precursor pool.

approximately 60 hpf, the larval pigment pattern is established with approximately 460 post-mitotic melanocytes. This number of larval melanocytes remains nearly constant, with only minimal birth and death of melanocytes occurring, until the onset of adult pigment pattern metamorphosis at 14 days postfertilization (dpf) (Milos and Dingle, 1978; Johnson et al., 1995) (reviewed by Rawls et al., 2001). Previously, we demonstrated the homeostatic regulation of larval melanocytes by larval melanocyte regeneration following melanocyte ablation with a dermatology laser. We further revealed that this melanocyte regeneration is achieved through the recruitment of undifferentiated cells, which tends to exclude division of differentiated melanocytes (i.e. compensatory regeneration, Fig. 1B) as the mechanism for larval melanocyte regeneration (Yang et al., 2004). Despite the power of such laser ablation, our attempts to further investigate the mechanisms of larval melanocyte regeneration were hampered by the limiting number of regenerating melanocytes that could be generated for thorough analyses of cell division events.

In this study, we have developed a pharmacological method to ablate the entire melanocyte population in zebrafish larvae. This now allows us to further test the mechanisms underlying melanocyte regeneration. We show that a small molecule, (2-morpholinobutyl)-4-thiophenol (MoTP), specifically ablates melanocytes or melanoblasts, and that the melanocytotoxicity is mediated via tyrosinase activity, presumably to convert MoTP to cytotoxic quinone species. Following MoTP treatment, we demonstrate by BrdU incorporation experiments that regenerated melanocytes are derived from the division of otherwise quiescent melanocyte precursors or stem cells. We further show that this regeneration requires the *kit* receptor tyrosine kinase. Together with our analyses of melanocyte regeneration in wild-type and *kit*^{j1e99} animals, we suggest that, in addition to establishing the larval melanocyte pattern, embryos set aside a small number of reserve cells (melanocyte precursors or stem cells) with an uneven distribution. These cells can be drawn upon to re-enter developmental pathways, divide multiple times and reconstitute the larval melanocyte population following melanocyte ablation by MoTP treatment.

MATERIALS AND METHODS

Stocks

Zebrafish were reared according to standard protocols at 28.5°C, unless otherwise noted (Westerfield, 1993). All developmental staging is reported in hours and days postfertilization (hpf and dpf, respectively), corresponding to staging at the standard temperature of 28.5°C. Staging at permissive temperature (25°C) is translated to 28.5°C stages as previously described (Kimmel et al., 1995). *kit*^{j1e99} and *fms*^{j4e1} have been previously described (Rawls and Johnson, 2003; Parichy et al., 2000). *sdy*^{j9s1} is a spontaneous, homozygous viable allele of the *shady* locus (Kelsh et al., 1996) that has approximately 10% of the normal number of embryonic or larval iridophores (C.-T.Y., unpublished). All references to these mutant alleles correspond to homozygous animals.

Chemicals

(2-morpholinobutyl)-4-thiophenol (MoTP) was custom synthesized by Gateway Chemical Technology (St Louis, MO). 4-hydroxyanisole (4-HA) (or 4-methoxyphenol) was purchased from Sigma-Aldrich (M1865-5, St Louis, MO). The dose responses of both chemicals in melanocytotoxicity and fish lethality were tested, and the most melanocytotoxic concentrations with low fish lethality were chosen for zebrafish melanocyte ablation experiments. MoTP and 4-HA were dissolved in dimethyl sulfoxide (DMSO) to make stock solutions, which were then diluted in egg water at 14 μg/ml (50 μM) and 2 μg/ml (16 μM) final concentrations, respectively. For phenylthiourea (PTU) treatment, 0.1-0.2 mM PTU was added to egg water and changed every 2 days (Milos and Dingle, 1978).

Whole-mount in situ hybridization

In situ hybridization with antisense digoxigenin (DIG)-labeled riboprobes was performed as described (Jowett and Yan, 1996), using 68°C hybridization and stringency washes, alkaline phosphatase-conjugated secondary antibodies and NBT/BCIP (Roche, Indianapolis, IN). The riboprobes of *mitf* [*microphthalmia-associated transcription factor* (Lister et al., 1999)], *kit* [*kit receptor tyrosine kinase* (Parichy et al., 1999)] and *dct* [*dopachrome tautomerase* (Kelsh et al., 2000)] were previously described. A partial *tyrosinase* (*tyr*) cDNA (Page-McCaw et al., 2004) was obtained by RT-PCR with primers 5′-CATCATCATGTCTCTCCATCTCC-3′ and 5′-CAGCATAATGCTTGCATCCTTC-3′, and cloned into a pBluescript SK vector (Strategene) for riboprobe synthesis. For in situ hybridization performed on larval samples older than 72 hpf, larvae were fixed in 4% paraformaldehyde (PFA) with 1% DMSO overnight, and probes were fragmented to ~300 nucleotides (Parichy et al., 2003). For some rounds of staining (Figs 2, 3), normally reared embryos were treated with 0.1-0.2 mM PTU to completely block melanin synthesis, thereby allowing easier visualization of NBT/BCIP precipitates in otherwise dark melanocytes. Note that *dct*$^{+}$ melanoblasts are first detected at 19 hpf and they remain *dct*$^{+}$ and lack melanin for approximately 5 hours, until the beginning of melanogenesis at 24 hpf (Kelsh et al., 2000). *dct* expression continues to be detected within the pigmented melanocytes through 72 hpf. Therefore, in our experiments (Fig. 3), melanin production was blocked by PTU for easier visualization and photography of *dct* expression; the *dct*$^{+}$ cell counts show both *dct*$^{+}$ melanoblasts and differentiated (but PTU-masked) melanocytes.

BrdU incorporation and detection

To detect and quantify cell division events in melanocyte lineages during larval melanocyte regeneration, normally reared and MoTP-treated larvae at various developmental stages were immersed in a solution of 5-bromo-2′-deoxyuridine (BrdU; 5 mM) for 24 hours in pulse labeling experiments. In the continuous labeling experiment, we changed the BrdU solution every 24

hrs. At the harvest stages, animals were fixed, imbedded in paraffin wax, and then cut into series of 5-μm-thick sagittal sections. Sections were deparaffinized and incubated with mouse anti-BrdU monoclonal antibody (1:300 dilution, Santa Cruz), followed by a secondary incubation with Alexa Fluor 594-conjugated goat anti-mouse Ig (1:300 dilution, Molecular Probes), and bisbenzimide (100 ng/ml; Sigma) for nuclear staining (Rawls et al., 2004). BrdU incorporation was determined by first identifying bisbenzimide-positive nuclei (blue fluorescence) in pigmented melanocytes, then assessing BrdU incorporation (red fluorescence) in each identified nucleus (Fig. 5).

RESULTS

Melanocyte differentiation proceeds to *tyr*$^+$ and *dct*$^+$ stages in the presence of MoTP

To identify a chemical that ablates the entire larval melanocyte population, we sought to investigate the biological effect of MoTP in zebrafish melanocyte development. MoTP was first described in a small molecule screen for drugs that affect zebrafish development (Peterson et al., 2000). These researchers observed that embryos developing in the presence of MoTP lacked body melanocytes, whereas their retinal pigment epithelium (RPE) was lightly pigmented. This differential effect on RPE and neural crest (NC)-derived melanocytes suggests that MoTP does not merely block general melanin production, for instance as does a tyrosinase inhibitor such as PTU. Furthermore, Peterson et al. reported that when larvae were removed from MoTP after a three-day incubation, melanocytes gradually repopulated the larval body during the ensuing two days. Together, these observations led to the suggestion that MoTP reversibly blocks or delays NC melanocyte development in zebrafish (Peterson et al., 2000).

To test the hypothesis that MoTP causes developmental delay in the melanoblast lineages, we examined their development in MoTP-treated larvae by performing a series of whole-mount RNA in situ hybridization with the early stage melanoblast markers *mitf* (Lister et al., 1999) and *kit* (Parichy et al., 1999), and the late stage melanoblast markers *tyr* (Page-McCaw et al., 2004) and *dct* (Kelsh et al., 2000) (C.-T.Y., unpublished). For these experiments, we incubated 14 hpf embryos in 14 μg/ml MoTP solution and fixed them at 27 hpf for in situ analysis. Following in situ hybridization, we were unable to distinguish differences in the developmental patterns or numbers of labeled cells in MoTP-treated larvae compared with untreated larvae for each of the markers (Fig. 2A-H). These results indicate that the differentiation of NC-derived melanoblasts remains normal and proceeds to late developmental stages (*tyr*$^+$ or *dct*$^+$) in the presence of MoTP. Interestingly, untreated late-stage melanoblasts typically begin to melanize prior to 27 hpf, but in MoTP treated larvae, this terminal marker (melanin) fails to form.

MoTP is cytotoxic to larval melanocytes

Because our foregoing analysis revealed that MoTP-treated melanoblasts proceed to late stages of differentiation but fail to reach their terminal stage of melanin production, we next explored their fate at subsequent developmental periods in MoTP-treated larvae. We found that the number of *dct*$^+$ cells in treated larvae declined from a maximum of 100 at 31 hpf to an average of 15 *dct*$^+$ cells by 60 hpf (Fig. 3B,D,F-H). By contrast, in the untreated larvae, the number of *dct*$^+$ cells steadily increased to more than 300 during the same time period (Fig. 3A,C,E,H). Note that the majority of the *dct*$^+$ cells in the untreated larvae are differentiated melanocytes, whose subsequent melanin production was blocked by incubation with PTU, allowing for easier visualization of the in situ marker (see Materials and methods). The disappearance of *dct*$^+$ cells in treated larvae raised the possibility that, in the presence of MoTP, melanoblasts reach the *tyr* and *dct* expression stage, at which time they become sensitive to MoTP and die.

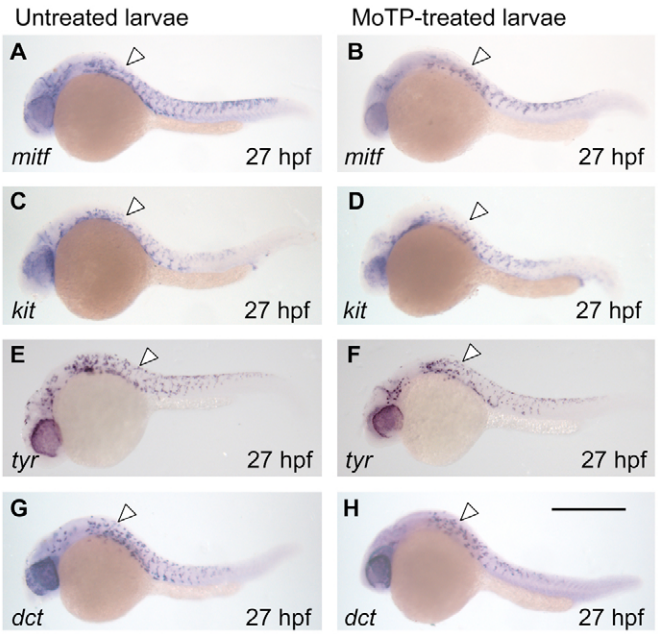

Fig. 2. Melanocyte lineages develop to late stages in the presence of MoTP. (**A-H**) The development of melanocyte lineages in MoTP-treated (B,D,F,H) and untreated (A,C,E,G) larvae were examined by whole-mount RNA in situ hybridization with *mitf* (A,B), *kit* (C,D), *tyr* (E,F) and *dct* (G,H). For these experiments, embryos were incubated in MoTP solution from 14 to 27 hpf, then immediately fixed for in situ analysis. The developmental patterns and the numbers of cells (white arrowheads) for each of the markers are indistinguishable in the MoTP-treated larvae from those in untreated larvae. Untreated larvae were reared in PTU to completely block melanin synthesis, thereby allowing easier visualization of NBT/BCIP precipitates in melanocytes. Scale bar: 500 μm.

We explored the notion that MoTP ablates cells in the melanocyte lineages by observing its effects on melanocytes that were first allowed to melanize in the absence of MoTP. When 48 hpf larvae with pigmented melanocytes were incubated in MoTP solution, larval melanocytes became punctate within 12 hours (Fig. 4A-D), and, by 24 hours, these punctate melanocytes began to extrude from the epidermis (Fig. 4E). As these two phenotypes are hallmarks of melanocyte cell death in fish (Parichy et al., 1999; Sugimoto et al., 2000), we interpret these results to indicate that MoTP induces melanocyte cell death.

The melanocytotoxicity of MoTP is dependent on tyrosinase activity

We sought to investigate the mechanism underlying MoTP cytotoxicity in melanocytes. One class of phenolic compounds has been previously reported to cause cytotoxicity specific to melanocytes (melanocytotoxicity) in mammals (reviewed by Riley, 1985). These compounds feature a phenolic ring with a functional group at the para position, a structure that is similar to tyrosine, the initial substrate of tyrosinase during the biochemical synthesis of melanin. Biochemical studies have suggested that this class of phenolic compounds, such as 4-hydroxyanisole (4-HA; Fig. 4G), competes with tyrosine for hydroxylation by tyrosinase and, consequently, is converted to a cytotoxic form, mainly o-quinone,

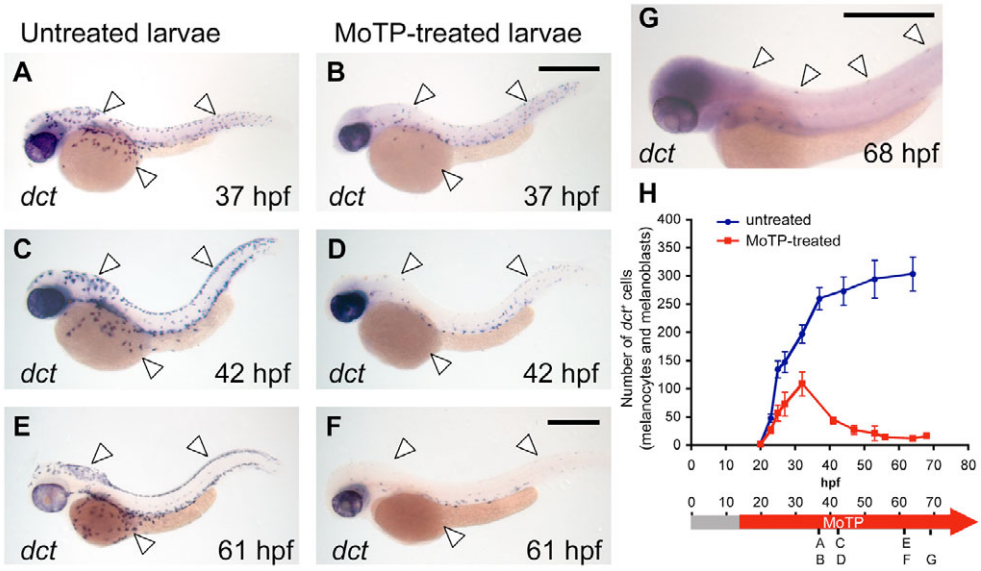

Fig. 3. The number of *dct*⁺ cells declines in the presence of MoTP. (**A-H**) The development of late-stage *dct*⁺ cells was further examined as the MoTP incubation continued. Larvae were reared in MoTP solution beginning at 14 hpf and fixed at selected developmental stages up until 68 hpf for in situ analysis. (A,C,E) The distribution and the number of *dct*⁺ cells in untreated larvae (reared in PTU solution) at 37, 42 and 61 hpf, respectively. Note that many *dct*⁺ cells in the untreated animals are differentiated melanocytes that remain unpigmented as a result of PTU treatment. (B,D,F) *dct*⁺ cells in the MoTP-treated larvae at 37, 42 and 61 hpf, respectively, revealing a gradual disappearance of *dct*⁺ cells during the MoTP incubation. The number of *dct*⁺ cells in the MoTP-treated larvae begins to decline from a maximum of ~100 *dct*⁺ cells at 31 hpf to an average of 15 *dct*⁺ cells by 60 hpf (red line in H). These *dct*⁺ cells have a stereotyped spacing pattern in the dorsum (white arrowheads in G). By contrast, the number of *dct*⁺ cells steadily increases to more than 300 in the untreated larvae (blue line in H). Scale bar: in B, 500 μm for A-D; in F, 400 μm for E,F; in G, 400 μm.

which is associated with the initiation of cellular damage in melanocytes (Riley, 1975; Naish et al., 1988). Thus, these studies demonstrated that the melanocytotoxicity of such phenolic compounds is mediated by tyrosinase activity (Fig. 4I). Like known members of this class of phenolic compounds, MoTP also has a phenolic ring with a functional group, in this case (morpholinobutyl)-thio, at the para position. Therefore, we sought to test whether MoTP acts similarly to the 4-HA-related class of phenolic compounds. If so, we reasoned that the chelation of copper, an essential cofactor for tyrosinase activity, by addition of the copper chelator PTU, should block the melanocytotoxicity of MoTP (Fig. 4I). Accordingly, we co-incubated 48 hpf larvae in MoTP solution with 0.1-0.2 mM PTU. We found that the melanocytotoxicity of MoTP was completely suppressed in the presence of PTU, as lightly pigmented and dendritic melanocytes were observed, but we observed no evidence of punctate melanocytes or their subsequent extrusions in these larvae (Fig. 4F).

To further demonstrate that the melanocyte cell death caused by MoTP is related to the melanocytotoxicity described for 4-HA, we tested the effects of 4-HA in zebrafish. When embryos were reared

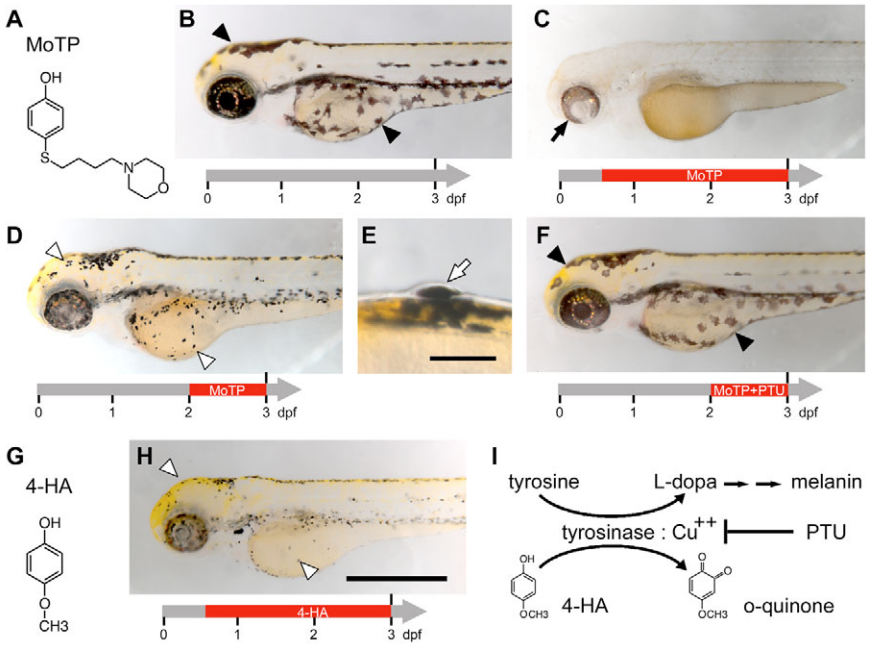

Fig. 4. The melanocytotoxicity of MoTP is mediated by tyrosinase activity. (**A**) The chemical structure of (2-morpholinobutyl)-4-thiophenol (MoTP). (**B**) Dendritic (healthy) melanocytes (black arrowheads) in an untreated larva at 3 dpf. (**C**) When larvae were incubated in MoTP solution from 14 to 72 hpf, no neural crest-derived melanocytes were observed, but RPE is lightly pigmented (black arrow). (**D**,**E**) When 48 hpf larvae with pigmented melanocytes were shifted to MoTP, within 24 hours, larval melanocytes had become punctate (white arrowheads in D) and began to extrude from the epidermis (white arrow in E), a hallmark of melanocyte cell death. (**F**) The melanocytotoxicity of MoTP was blocked by PTU, as indicated by the dendritic appearance of lightly pigmented melanocytes (black arrowheads in F) following co-incubation of MoTP and PTU from 48 to 72 hpf. (**G**) The chemical structure of 4-hydroxyanisole (4-HA). (**H**) When larvae were incubated with 4-HA from 14 to 72 hpf, the same punctate melanocyte pattern of cell death appeared (white arrowheads). (**I**) Illustration of the mechanism of 4-HA melanocytotoxicity (see Riley, 1985). Note that tyrosinase converts the prodrug 4-HA to a cytotoxic o-quinone. Because copper is an essential cofactor for tyrosinase, its activity is blocked by co-incubation with PTU, a copper chelator. Timelines (gray) below the panels indicate the period of drug treatments (red) and analysis time (vertical line above timelines). Scale bars: in H, 500 μm for B-D,F,H; in E, 50 μm.

in 2 μg/ml 4-HA solution (14-72 hpf), the same punctate melanocyte patterns of cell death were observed as we described following MoTP treatment (Fig. 4H). In addition, the melanocytotoxicity of 4-HA was abrogated by co-incubation with PTU (data not shown). These results suggest that MoTP acts by the same, or a similar, mechanism as 4-HA conversion from a prodrug into a cytotoxic form by the activity of tyrosinase, an enzyme found at high levels in melanocytes.

Melanocyte regeneration following MoTP-induced ablation

As described above, incubating zebrafish embryos in MoTP results in the loss of melanoblasts or melanocytes. By 72 hpf, when untreated larvae have established the larval melanocyte pattern, MoTP-treated larvae lack all melanocytes. When MoTP-treated larvae are transferred to fresh egg water at 72 hpf, melanocytes gradually develop over the next 4-5 days (as described in the ensuing sections). Such regeneration of larval melanocytes now provides an opportunity to explore how regenerating cells are derived from their precursors, including the role for cell division and differentiation state of precursors (below).

Melanocytes regenerate from the division of undifferentiated melanocyte precursors following MoTP treatment

We first sought to test whether, following melanocyte ablation by MoTP, melanocytes regenerate through mechanisms involving cell division. Accordingly, we incubated larvae in MoTP from 4-5 dpf, to ablate differentiated melanocytes. We also incubated these larvae continuously in BrdU from 4-10 dpf, to reveal whether the differentiated melanocytes that arise have undergone rounds of DNA synthesis, BrdU incorporation, and thus, cell division. Counting the percentage of BrdU-positive, melanin-positive melanocytes in 5 μm paraffin sagittal sections at 10 dpf (5 days post-MoTP treatment) showed that 97.2±2.5% of regenerated melanocytes are BrdU positive, compared with only 3.9±3.5% BrdU-positive melanocytes in untreated animals (Fig. 5). This finding indicates that virtually all regenerated melanocytes develop from precursors that have undergone one or more rounds of cell division following MoTP-induced melanocyte ablation.

We next explored models of regeneration that do not involve cell division (Fig. 1C,D). We reasoned that if the embryo sets aside late-stage precursors that could differentiate directly into melanocytes without cell division for regeneration and regulation (Fig. 1D), these late stage precursors might express a late-stage melanoblast marker, such as *dct*, in untreated (non-regenerating) larvae. In situ analysis of *dct* expression showed very few dorsal *dct*$^{+}$ melanoblasts (0.2-0.3 per animal) in untreated fish between 74 and 128 hpf (Fig. 6C). By contrast, in MoTP-treated larvae (14-72 hpf), we detected 8- to 20-fold more dorsal *dct*$^{+}$ melanoblasts (two to three per animal) at the same developmental stages (Fig. 6A-C). This result indicates that large numbers of late-stage (*dct*$^{+}$) melanoblasts are not available for regenerating the larval melanocyte pattern, and also that ablation of the embryonic melanoblasts and melanocytes results in the recruitment of *dct*$^{+}$ melanoblasts from less-differentiated precursors during melanocyte regeneration.

An alternative model of regeneration without cell division is regeneration by transdifferentiation from one differentiated cell type to another. For example, in amphibians, other NC-derived chromatophores have been suggested to transdifferentiate into melanophores under various experimental conditions (Thidaudeau and Holder, 1998; Ide and Akira, 1988); thus, differentiated iridophores and xanthophores may be candidates for transdifferentiation into melanocytes in this regeneration system (Fig. 1C). Evidence for or against such transdifferentiation might be gained by assessing regeneration in the absence of iridophores or xanthophores. Accordingly, we investigated whether melanocyte regeneration occurred in mutant larvae that lacked most or all iridophores (*sdy*^{j9s1}) or xanthophores (*fms*^{j4e1}), but that have a normal embryonic and larval melanocyte pattern. In each mutant, following melanocyte ablation by MoTP treatment (14-72 hpf), we observed that melanocyte regeneration occurred identically to that in wild-type larvae (data not shown), which suggests that transdifferentiation from iridophores and xanthophores is not responsible for melanocyte regeneration. We note, however, that these results do not exclude the possibility of transdifferentiation from other cell types.

Taken together, these results suggest that regenerated melanocytes arise by the recruitment of undifferentiated melanocyte precursors that then divide several times and differentiate into new melanocytes.

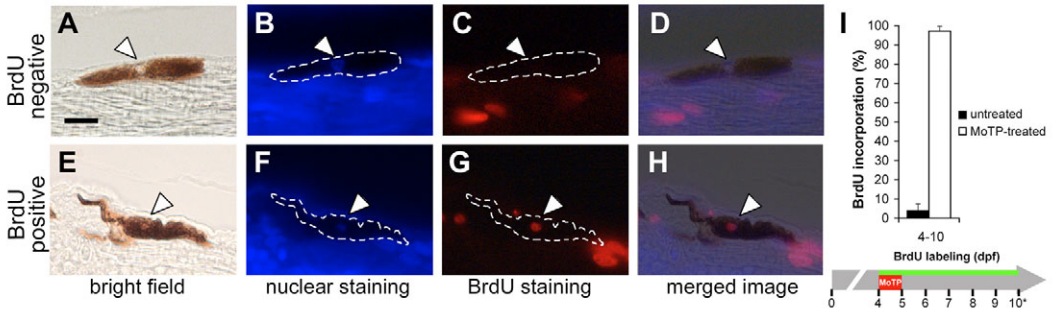

Fig. 5. Larval melanocyte regeneration following MoTP treatment is achieved by cell division. (**A-H**) Cell division events in melanocyte lineages during larval melanocyte regeneration were tracked by BrdU incorporation experiments. Larvae were continuously incubated in BrdU (5 mM) during and after MoTP treatment, then fixed, paraffin embedded and 5 μm sagittal sections processed for BrdU immunohistochemistry after melanocyte regeneration was mostly completed at 10 dpf (5 days post-MoTP treatment). BrdU incorporation states of pigmented melanocytes were assessed by first identifying melanocyte nuclei (thinning in melanin, white arrowheads in A and E) accompanied by bisbenzimide staining (white arrowheads in B and F). These were then examined for red fluorescence indicative of BrdU incorporation (white arrowheads in C and G). D is the overlay image of A, B and C, indicating a melanocyte that did not incorporate BrdU during the BrdU labeling, whereas in H, the overlay image of D, E and F shows a different melanocyte that did incorporate BrdU during the BrdU labeling. (**I**) Quantitative analyses of BrdU incorporation in larvae exposed to MoTP from 4 to 5 dpf. Black and white bars indicate BrdU incorporation in untreated and MoTP-treated larvae, respectively. Horizontal green line indicates periods of BrdU labeling. Asterisk in I indicates the developmental stages at which larvae were sacrificed for BrdU incorporation analysis. Scale bar in A: 10 μm for A-H.

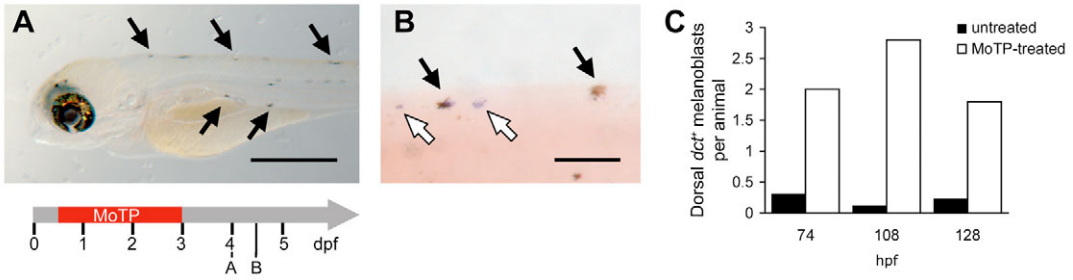

Fig. 6. Appearance of *dct*⁺ melanoblasts following MoTP-induced melanocyte death. (**A**,**B**) Timeline for A and B is shown below A. Lightly pigmented, new melanocytes (black arrow; A,B) and *dct*⁺ melanoblasts (white arrows, B) appear 24-36 hours postMoTP treatment. (**C**) The appearance of the *dct*⁺ melanoblasts in the dorsal stripe is specifically induced in the MoTP-treated larvae, average of two to three *dct*⁺ melanoblasts per animal examined (white bars), compared with less than 0.3 *dct*⁺ melanoblasts (black bars) at equivalent stages in untreated larvae. Eight to 18 animals were analyzed for each bar. Scale bars: in A, 500 μm; in B, 100 μm.

Our results tend to exclude possible regeneration from differentiated melanocytes (Yang et al., 2004), iridophores or xanthophores, or from late-stage (*dct*⁺) precursors.

Dynamics of regenerated melanocyte precursor cell division

We were interested in the dynamics of the cell division during larval melanocyte regeneration. Accordingly, following MoTP incubation (14-72 hpf) to ablate the ontogenetic melanocyte population, we monitored the history of cell division by pulse-labeling regenerated melanocytes with BrdU for 24 hours at various regeneration stages, and assessed the percentage of BrdU-positive melanocytes at 8 dpf (5 days post-MoTP treatment). We found that approximately 35-40% of melanocytes incorporated BrdU on each of the second and third days post-MoTP treatment. The percentage of melanocytes that had incorporated BrdU during the labeling period then declines to approximately 20% by the fourth and fifth days post-MoTP treatment. By contrast, we found that only 5-8% of melanocytes in the untreated larvae incorporated BrdU at the equivalent developmental stages (Fig. 7A). These results suggest that cell divisions in melanocyte precursors occur continuously throughout the 5 days of regeneration.

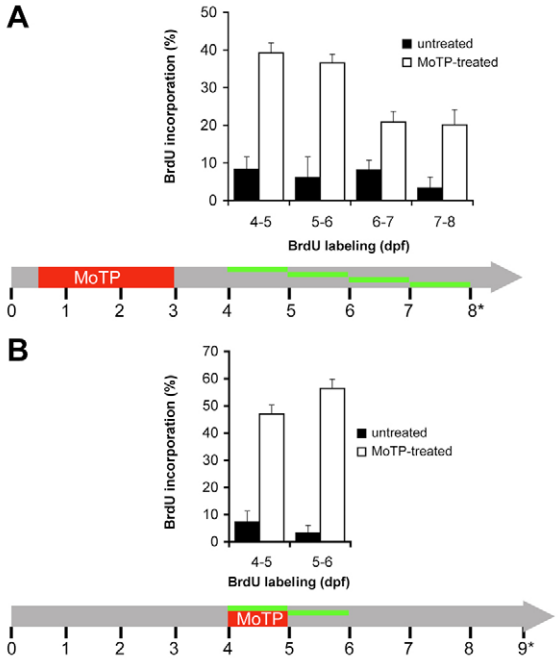

Fig. 7. Dynamics of cell divisions during melanocyte regeneration. (**A**,**B**) The history of cell divisions in melanocyte lineages during larval melanocyte regeneration was determined by pulse-labeling with BrdU for 24 hours at various stages during or after MoTP treatment. Quantitative analyses of BrdU incorporation were conducted in larvae exposed to MoTP from 14 to 72 hpf (A), or 4 to 5 dpf (B). Black and white bars indicate BrdU incorporation in untreated and MoTP-treated larvae, respectively. Horizontal green lines indicate periods of BrdU labeling. Asterisks in A and B indicate the developmental stages at which larvae were sacrificed for BrdU incorporation analysis.

We further investigated how rapidly melanocyte precursors or stem cells are induced to re-enter the cell cycle upon melanocyte ablation by MoTP treatment. Because we found that we could not achieve reliable BrdU incorporation in zebrafish larvae by simply rearing larvae in BrdU solution prior to 4 dpf, we instead used a later stage for MoTP melanocyte ablation. Accordingly, we ablated larval melanocytes by MoTP treatment from 4 to 5 dpf, incubated larvae with BrdU during the 4 to 5 and 5 to 6 dpf periods, and then assessed BrdU incorporation in melanized melanocytes after regeneration was near completion at 9 dpf. We found that 47% of melanocytes had incorporated BrdU during the 4 to 5 dpf labeling period (coincident with the MoTP treatment), rising to 56% BrdU-positive melanocytes during the 5 to 6 dpf period (Fig. 7B). These results indicate that melanocyte precursors or stem cells are induced to enter the cell cycle within 24 hours of the beginning of MoTP incubation. Because signs of melanocyte cell death occur as early as 12 hours after the beginning of MoTP exposure, we suggest that this induction may begin less than 12 hours after melanocyte cell death.

Recruitment of melanocyte precursors or stem cells in wild-type and mutant animals

We were also interested in the distribution of quiescent melanocyte precursors or stem cells that contribute to melanocyte regeneration following melanocyte ablation by MoTP treatment. Ideally, this knowledge could be gained by examining markers for the melanocyte stem cells. Lacking such stem cell markers, we have instead examined the distribution of differentiated melanocytes in wild-type and mutant animals for less direct inferences. Thus, in wild-type animals, we observed the first appearance of regenerated melanocytes 24 hours post-MoTP treatment. The number of melanocytes continues to steadily rise for the ensuing 4 days and reaches a plateau of approximately 350-400 melanocytes by 9 dpf (6 days after the removal of MoTP). This number reveals a deficit

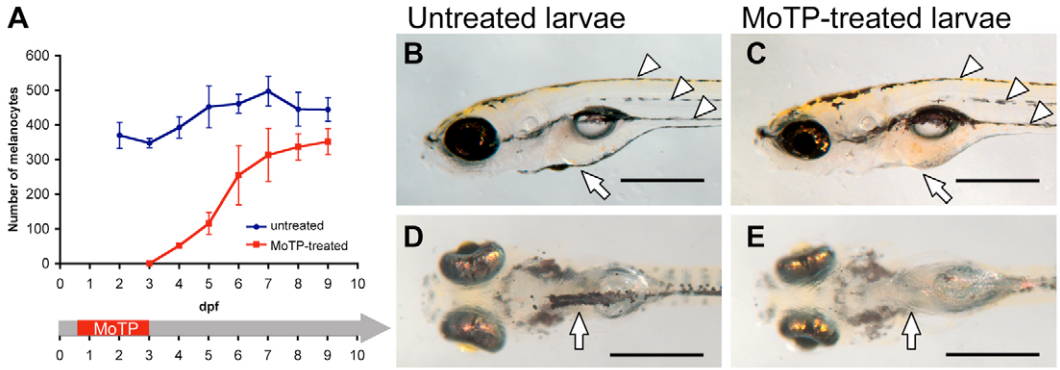

Fig. 8. Ventral yolk sac melanocytes fail to regenerate following melanocyte ablation by MoTP treatment. (**A**) Larval melanocytes were counted in the untreated larvae (blue line) and MoTP-treated (14-72 hpf) larvae (red line). After the appearance of melanocytes at 24 hours post-MoTP treatment, the number of melanocytes continues to steadily rise in the ensuing 4 days and then plateaus at approximately 350-400 melanocytes by 9 dpf (6 days after removal of MoTP). (**B-E**) At this stage of melanocyte regeneration, MoTP-treated larvae (C,E) have regenerated almost identical pigment patterns to those of the untreated larvae (B,D), with a similar number and distribution of melanocytes in the dorsal, lateral and ventral larval melanocyte stripes (white arrowheads). However, MoTP-treated larvae fail to regenerate the majority of the ventral yolk sac melanocytes (white arrow in C and E). Scale bars: 500 μm.

of approximately 60-110 melanocytes in MoTP-treated versus untreated larvae (average 460 melanocytes; Fig. 8A). To further explore this deficit, we examined the patterns of melanocytes in the MoTP-treated and untreated larvae at 9 dpf. We found MoTP-treated larvae regenerate an almost identical pigment pattern compared to that of the untreated larvae, with a similar number and distribution of melanocytes in the dorsal, lateral and ventral larval melanocyte stripes. One exception was that MoTP-treated larvae failed to regenerate the majority of the ventral yolk sac melanocytes (Fig. 8B-E). Typically, untreated larvae have approximately 65 melanocytes in the ventral yolk sac stripe at this stage; therefore, the absence of those melanocytes in MoTP-treated larvae accounts for the observed melanocyte deficit (Fig. 8A). When we allowed these MoTP-treated larvae to develop to stages immediately prior to the onset of adult pigment pattern metamorphosis, we observed that melanocytes slowly begin to repopulate the ventral yolk sac area, resulting in approximately 35% of the normal number of ventral yolk sac stripe melanocytes by 14 dpf (11 days post-MoTP treatment; data not shown). These results suggest either that the region of the ventral yolk sac is devoid of quiescent melanocyte precursors or stem cells, or that they are less responsive to the presence or absence of differentiated melanocytes in this area (see Discussion).

To further understand the mechanisms by which melanocyte homeostasis is regulated by quiescent melanocyte precursors or stem cells, we examined melanocyte regeneration in mutants for *kit*, which has been suggested to play important roles in the recruitment of melanocyte stem cells or expansion of melanoblasts (Rawls and Johnson, 2001). The *kit* receptor tyrosine kinase is required for ontogenetic melanocyte development in zebrafish embryos. In kit^{b5} (a null mutation) embryos, NC-derived melanocytes differentiate, but fail to migrate to proper locations and subsequently undergo programmed cell death, resulting in larvae devoid of melanocytes until pigment pattern metamorphosis (Johnson et al., 1995; Parichy et al., 1999). Previously, by using a temperature-sensitive allele, kit^{j1e99}, at the restrictive temperature (30-33°C), we showed that *kit* is also required to fill in gaps in the larval melanocyte pattern created by laser ablation. Interestingly, kit^{j1e99} animals also failed to regenerate melanocytes after laser ablation at temperatures described as permissive for embryonic melanocyte development or for melanocyte regeneration in the regenerating adult caudal fin (23 or 25°C) (Yang et al., 2004; Rawls and Johnson, 2001; Rawls and Johnson, 2003). Because the laser ablations resulted in animals with only small regions devoid of melanocytes, we revisited the role of kit^{j1e99} in larval melanocyte regeneration using MoTP treatment to ablate all the melanocytes in the larvae. When we reared kit^{j1e99} animals in MoTP solution (14-72 hpf) at the permissive temperature (25°C), we found that new melanocytes appeared significantly more slowly than in wild-type larvae after MoTP treatment (Fig. 8A, Fig. 9A), achieving a plateau of 15.9±5.7 melanocytes at 9 dpf. We discuss the inferences that can be drawn from the number and distribution of these few regenerated melanocytes more extensively below (see Discussion).

DISCUSSION

Zebrafish melanocyte ablation by MoTP

To complement the traditional regeneration studies of vertebrate appendages or organs, we have developed methods to ablate a single cell type, the melanocyte, and analyze its regeneration in zebrafish larvae. Previously, we have shown that a standard, hand-held dermatology laser can be used to specifically ablate melanocytes from small regions of zebrafish larvae, allowing us to study melanocyte regeneration in otherwise intact animals (Yang et al., 2004). Here, we have developed a different method, which can ablate the entire melanocyte population in zebrafish larvae. We demonstrated that a small molecule, MoTP, is cytotoxic to late stage melanoblasts and melanocytes in zebrafish larvae, and that this melanocytotoxicity is dependent on tyrosinase activity. The melanocyte specificity of MoTP ablation is also stage specific; we found that exposure of larvae to MoTP after 5 dpf had no effect on melanocytes (data not shown), presumably because of the decline of tyrosinase activity in mature melanocytes. Although tyrosinase is also expressed in the RPE (Camp and Lardelli, 2001), we found that the RPE is relatively insensitive to MoTP-induced cell death, as the RPE develops normally, albeit with lighter pigment, at the MoTP concentration that causes NC-derived melanocyte cell death (Fig. 4C). This differential sensitivity between types of melanocyte could result from differential tyrosinase expression or activity, or possibly from differences in the accessibility of these cells to MoTP during the treatment.

A similar melanocytotoxicity has been described for a related class of compound, including 4-HA. Like MoTP, 4-HA is a prodrug that is converted by tyrosinase to a cytotoxin. In the case of 4-HA, the cytotoxic product is o-quinone (Naish et al., 1988). Thus, we predict that tyrosinase converts MoTP to a similar molecule. The melanocytotoxicity of 4-HA was explored for use in melanoma chemotherapy, but discontinued because of severe liver damage resulting from liver cytochrome P450 conversion of 4-HA to toxic p-quinone (Rustin et al., 1992; Moridani et al., 2002). The difference in structure of MoTP from 4-HA in the functional group at the para position raises the possibility that MoTP or related derivatives may not show the same liver toxicity. The recent development of a melanoma model in zebrafish may provide a useful platform for evaluating MoTP as a chemotherapeutic, or for the search for other tyrosinase-dependent prodrugs for the treatment of melanoma (Patton et al., 2005).

In addition, the finding that MoTP is a prodrug converted by tyrosinase to a cytotoxic form suggests the potential application that specific and non-invasive ablation of any cell type in complex tissues or organs can be achieved by expressing tyrosinase under the control of cell- or tissue-specific promoters, then exposing the fish to MoTP. A similar use for transgenic expression of a prodrug converting enzyme, which we are exploring, is expression of bacterial nitroreductase in specific cells (Medico et al., 2001) (M. T. Saxena and S. L. Johnson, unpublished), followed by exposure to bacterial enzyme-specific substrates metronidazole or CB1954, that in turn are converted to cytotoxins.

We note that Harris et al. (Harris et al., 2003) have previously demonstrated an example of single cell type ablation by small molecules in zebrafish; aminoglycoside antibiotics, including neomycin, can induce hair cell death in larval zebrafish lateral line neuromasts, which is then followed by hair cell regeneration.

Larval melanocyte regeneration is achieved via the division of otherwise quiescent melanocyte precursors

We explored the developmental mechanisms by which melanocytes regenerate following melanocyte ablation by MoTP treatment, particularly in regards to the role of cell division and the differentiated state of the regeneration precursor cells (Fig. 1). The finding that melanocyte regeneration occurs after essentially complete ablation of the larval melanocytes by MoTP, and our previous findings (Yang et al., 2004) that larval melanocytes regenerate from undifferentiated precursors, rather than differentiated melanocytes, following laser ablation, rule out that melanocyte regeneration is achieved via the proliferation of differentiated melanocytes (Fig. 1A). This finding, together with our finding that all or virtually all regenerated melanocytes arise via cell division after ontogenetic melanocyte ablation (Fig. 5I), provides strong support for the model outlined in Fig. 1B that larval melanocyte regeneration occurs via the recruitment of undifferentiated precursors to divide and then differentiate to produce the new larval melanocyte population (an example of epimorphosis).

Our findings also provide evidence against models of regeneration that do not involve cell division (Fig. 1C,D). The notion that late stage (*dct*$^{+}$) precursors are available to differentiate directly into melanocytes without cell division (Fig. 1D) is dispelled by our finding of few *dct*$^{+}$ melanoblasts in untreated larvae, especially when compared with the numbers of *dct*$^{+}$ melanoblasts found in MoTP-treated larvae (Fig. 6C). The notion of direct transdifferentiation (Fig. 1C) from other pigment cells playing a role in melanocyte regeneration is suggested by findings of transdifferentiation between chromotaphores in salamanders (Thidaudeau and Holder, 1998; Ide and Akira, 1988). However, our finding that *sdy* and *fms* mutants that lack most or all iridophores or xanthophores, respectively, regenerate melanocytes identically to wild-type larvae does not support the notion that melanocyte regeneration is derived from these other pigment cell types.

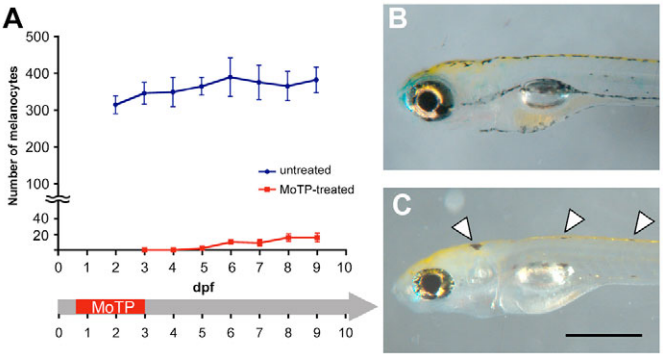

Fig. 9. Melanocyte regeneration deficit in *kit*^{j1e99} larvae. (**A**) Larval melanocytes were counted in the untreated (blue line) and MoTP-treated (14-72 hpf; red line) *kit*^{j1e99} larvae at the permissive temperature (25°C) for the temperature-sensitive allele. The first few melanocytes appear approximately 3 days post-MoTP treatment in the MoTP-treated *kit*^{j1e99} animals at 25°C. The number of melanocytes in MoTP-treated larvae reaches approximately 15 by 9 dpf (6 days after removal of MoTP, red line in A), whereas age-matched untreated *kit*^{j1e99} animals have approximately 350-400 melanocytes (blue line in A). (**B**,**C**) Note that the regenerated melanocytes exhibit a stereotyped spacing morphology in the dorsum (white arrowheads in C). B and C are untreated and MoTP-treated *kit*^{j1e99} larvae at 7 dpf, respectively. Scale bar: 500 μm

These studies show that melanocytes in larval zebrafish regenerate from undifferentiated precursors that may undergo several rounds of cell divisions prior to differentiation to replace the missing melanocyte pattern. It will be interesting to discover how much of this mechanism of recruiting undifferentiated precursors to reenter developmental pathways in this regeneration system is shared by the regulatory mechanism that acts in the embryo to precisely determine melanocyte number.

Melanocyte stem cells in zebrafish larvae

Homeostasis or regeneration of many tissues has been shown to be achieved via the recruitment of stem cells. Stem cells have two important characteristics: they are undifferentiated and they self-renew (Siminovitch et al., 1963). These two key characteristics of stem cells were elegantly demonstrated by multiple reconstitutions of hematopoietic cells in X-ray-irradiated mice (Spangrude et al., 1988). Because such techniques of transplantation and reconstitution are not generally possible for other lineages, other lines of evidence may help evaluate the notion of stem cells or quiescent precursors. The presence of melanocyte stem cells in zebrafish has been suggested by observations of the unlimited capacity of melanocyte pattern re-establishment in the regenerating caudal fin (Rawls and Johnson, 2000). Melanocyte or pigment cell stem cells have also been suggested to contribute to the adult melanocyte population during metamorphosis, indicating that stem cells are established during embryonic or larval stages (Johnson et al., 1995; Parichy, 2003). Assuming that each of these events draws upon the same precursor population, our finding of a high proliferative capacity of

the melanocyte precursors during larval melanocyte regeneration suggests that these melanocyte precursors have many of the characteristics expected of stem cells. Finally, the demonstration of melanocyte stem cells in mammalian hair follicles (Nishimura et al., 2002) supports the idea of an analogous stem cell in the zebrafish.

Zebrafish melanocytes begin to appear at 24 hpf, and the larval pigment pattern is established at approximately 60 hpf. Our results suggest that in addition to establishing the larval melanocyte pattern, embryos set aside a population of quiescent reserve cells, henceforth melanocyte stem cells, that can be drawn upon to generate new melanocytes for larval melanocyte homeostasis; for instance, for filling gaps in the melanocyte pattern (Yang et al., 2004), or for later stages of melanocyte development, such as for adult pigment pattern formation (Johnson et al., 1995; Parichy, 2003). Our BrdU incorporation experiments suggest that melanocyte stem cells are maintained in a minimal state of activity during the larval stage. Upon melanocyte ablation by MoTP treatment, melanocyte stem cells are released from this quiescent state, divide and produce new melanocytes to replenish the ablated population. The activity of these melanocyte stem cells and their descendant amplifying melanoblasts appears to be highly regulated during melanocyte regeneration. Our BrdU incorporation experiments show that the recruitment of melanocyte stem cells into the cell cycle is relatively rapid, beginning less than 24 hours after melanocyte cell death. Furthermore, we observe cell divisions throughout the 5-day regeneration period with fewer cell divisions at the end of this period (Fig. 7). The fact that the pattern is largely regenerated with no local excesses or deficits of melanocytes (with the exception of the ventral yolk sac stripe melanocytes, see discussion below) also suggests that feedback regulation from the final pattern regulates the later cell divisions.

One intriguing finding in our regeneration studies is that, following melanocyte ablation by MoTP treatment, ventral yolk sac stripe melanocytes fail to regenerate (Fig. 8). The melanocyte stripe on the ventral yolk sac is the last larval melanocyte stripe established, and, furthermore, these melanocytes migrate the largest distance from the dorsum to their final ventral locations. Uneven distribution of melanocyte progenitors has been described to account for the varying densities of melanoblasts in different parts of the mouse embryo (reviewed by Besmer, 1993; Wilkie et al., 2002). Following this logic, the failure of larval melanocyte regeneration in the zebrafish ventral yolk sac could be due to the lack of melanocyte stem cells in the region. Alternatively, melanocyte stem cells may in fact be established in the ventral yolk sac but fail to survey the environment for melanocyte homeostasis, or to re-enter developmental pathways upon the melanocyte ablation by MoTP treatment. Interestingly, one third of the normal number of ventral yolk sac stripe melanocytes eventually reappears by late larval stage, during the onset of adult pigment pattern metamorphosis (14 dpf, data not shown). An attractive possibility is that this late stage regeneration now takes advantage of melanocyte stem cells primed by the onset of pigment pattern metamorphosis to reconstitute the previously ignored yolk sac melanocyte deficit. Such models can be further tested once markers that label melanocytes precursors or stem cells are developed.

An interesting question of melanocyte regeneration is how many melanocyte stem cells in the zebrafish larvae contribute to the reconstitution of the entire larval melanocyte population following melanocyte ablation. One approach to answer this question is to estimate the number of cell divisions that each melanocyte has progressed through during regeneration. Based on our BrdU incorporation experiments, we estimate that melanocyte stem cells or the descendant amplifying melanoblasts may have gone through as many as two to four cell divisions. This is suggested in part by the accumulated percentage of BrdU-incorporated melanocytes observed over the six intervals of 24-hour BrdU labeling during and after MoTP incubation, indicating an average of 1.8 cell divisions for each melanocyte lineage (Fig. 7). This number of cell divisions per lineage is an underestimate, as some lineages are likely to have divided twice or more during any one period of 24-hour BrdU labeling. In addition, our observation that some melanocytes differentiate and leave the cell cycle during the early stage of regeneration suggests that those that differentiate at late stage of regeneration have undergone even more cell divisions. From these calculations, we estimate that there are approximately 35-145 melanocyte stem cells in larval zebrafish that give rise to the approximately 350-400 melanocytes present at the completion of regeneration.

Another estimate for the number of stem cells comes from our observation of *dct*-expressing cells during prolonged MoTP exposure. We typically observe 15-20 dct^+ cells in the larvae during prolonged MoTP incubation (50-68 hpf; Fig. 3H). In addition, the dct^+ cells on the dorsum of these larvae are distributed with a stereotyped spacing pattern (Fig. 3G). We suggest that these cells are newly progressed to dct^+ stage, and that they then die once sufficient MoTP-induced cytotoxins accumulate. An attractive possibility is that these dct^+ cells each mark the position or the domain of a single melanocyte precursor or melanocyte stem cell, and the that number of these dct^+ cells reflects the number of melanocyte stem cells. Because, at any given time, some stem cell lineages may not have dct^+ daughters, the number of melanocyte stem cells may be greater than the number of dct^+ cells present in a single fish at a particular moment.

Our study of larval melanocyte regeneration in kit^{j1e99}animals at permissive temperature may provide additional evidence for the above estimate of the number and position of melanocyte stem cells. Among its roles in melanocyte development, *kit* has been suggested to be required for melanoblast proliferation in mammals (Mackenzie et al., 1997). In zebrafish larvae, in addition to defects in melanocyte migration and subsequent survival, kit^{b5} null mutants also develop a reduced number of embryonic melanocytes (50-60% of the wild-type melanocyte number), consistent with a role in proliferation as well (Parichy et al., 1999). Here, we find that following melanocyte ablation and recovery at the otherwise permissive temperature for the allele, kit^{j1e99} animals regenerate approximately 5% (15.9±5.7) of the melanocyte number regenerated in wild-type animals (Fig. 9). The mutant lesion for this allele is in the second kinase domain (Rawls and Johnson, 2003), and seems to confer temperature-sensitivity on the gene product. The different effects of the kit^{j1e99} allele between ontogeny and regeneration may reveal a regeneration-specific function of the *kit* receptor tyrosine kinase mapping to this site, or, alternatively, that the mutation partially reduces *kit* function at the permissive temperature, and the regeneration role has a greater demand on *kit* activity. Whichever is the case, the distribution of melanocytes that regenerate in kit^{j1e99} animals may be informative of the distribution of melanocyte precursors or stem cells. We note that regenerated melanocytes in the dorsum of kit^{j1e99}animals are distributed in a similar pattern to the dct^+ cells observed in the prolonged MoTP-treated animals discussed above (Fig. 3G, Fig. 9C). One possibility is that each melanocyte stem cell gives rise to a single melanoblast that differentiates without further cell division. If this were so, then the number of regenerated melanocytes observed in the kit^{j1e99}animals may directly reflect the number, and possibly the position, of melanocyte stem cells.

Taken together, our observations on BrdU incorporation during regeneration, on the position and number of *dct*$^{+}$ cells during prolonged MoTP incubation, and on the position and number of regenerated melanocytes in *kit*^{j1e99} animals lead us to postulate that there are as few as 15, or as many as 145, quiescent melanocyte precursors or stem cells in the zebrafish larvae that contribute to the larval melanocyte regeneration described here.

Our finding that the roles of the *kit* receptor tyrosine kinase in the regeneration process are different from those previously described for the ontogenetic development of larval melanocytes now raises the possibility that the MoTP ablation and regeneration assay could be applied to forward genetic analysis. This may allow us to specifically isolate mechanisms involved in the regeneration process, including how the stem cell is kept in check by the presence of its target tissue, or how the stem cell is activated to re-enter the developmental pathway.

We thank Meera T. Sexena and John F. Rawls for critical reading of the manuscript. We would also like to acknowledge Charles Higdon and Steven Jacob for fish husbandry. The work was supported by National Institutes of Health Grant R01-GM 56988 to S.L.J.

References

Bach, J. F. (1994). Insulin-dependent diabetes mellitus as an autoimmune disease. *Endocr. Rev.* **15**, 516-542.
Besmer, P., Manova, K., Duttlinger, R., Huang, E. J., Packer, A., Gyssler, C. and Bachvarova, R. F. (1993). The kit-ligand (steel factor) and its receptor c-kit/W: pleiotropic roles in gametogenesis and melanogenesis. *Dev. Suppl*. 125-137.
Camp, E. and Lardelli, M. (2001). Tyrosinase gene expression in zebrafish embryos. *Dev. Genes Evol.* **211**, 150-153.
Chalkley, D. T. (1954). A quantitative histological analysis of forelimb regeneration in Triturus viridescens, *J. Morphol*. **94**, 21-70.
Cheng, H. and Leblond, C. P. (1974). Origin, differentiation and renewal of the four main epithelial cell types in the mouse small intestine. V. Unitarian Theory of the origin of the four epithelial cell types. *Am. J. Anat.* **141**, 537-561.
Compston, A. and Coles, A. (2002). Multiple sclerosis. *Lancet* **359**, 1221-1231.
Fuchs, E. and Raghavan, S. (2002). Getting under the skin of epidermal morphogenesis. *Nat. Rev. Genet.* **3**, 199-209.
Harris, J. A., Cheng, A. G., Cunningham, L. L., MacDonald, G., Raible, D. W. and Rubel, E. W. (2003). Neomycin-induced hair cell death and rapid regeneration in the lateral line of zebrafish (Danio rerio). *J. Assoc. Res. Otolaryngol*. **4**, 219-234.
Hay, E. D. and Fischman, D. A. (1961). Origin of the blastema in regenerating limbs of the newt Triturus viridescens. An autoradiographic study using tritiated thymidine to follow cell proliferation and migration. *Dev. Biol.* **3**, 26-59.
Holstein, T. W., Hobmayer, E. and David, C. N. (1991). Pattern of epithelial cell cycling in hydra. *Dev. Biol.* **148**, 602-611.
Ide, H. and Akira, E. (1988). Differentiation and transdifferentiation of amphibian chromatophores. *Prog. Clin. Biol. Res.* **256**, 35-48.
Johnson, S. L., Africa, D., Walker, C. and Weston, J. A. (1995). Genetic control of adult pigment stripe development in zebrafish. *Dev. Biol.* **167**, 27-33.
Jones, P. H. and Watt, F. M. (1993). Separation of human epidermal stem cells from transit amplifying cells on the basis of differences in integrin function and expression. *Cell* **73**, 713-724.
Jowett, T. and Yan, Y. L. (1996). Two-color whole-mount in situ hybridization. In *A Laboratory Guide to RNA: Isolation, Analysis, and Synthesis* (ed. P. A. Krieg), pp. 381-409. New York: John Wiley.
Kelsh, R. N., Brand, M., Jiang, Y. J., Heisenberg, C. P., Lin, S., Haffter, P., Odenthal, J., Mullins, M. C., van Eeden, F. J., Furutani-Seiki, M. et al. (1996). Zebrafish pigmentation mutations and the processes of neural crest development. *Development* **123**, 369-389.
Kelsh, R. N., Schmid, B. and Eisen, J. S. (2000). Genetic analysis of melanophore development in zebrafish embryos. *Dev. Biol.* **225**, 277-293.
Kimmel, C. B., Ballard, W. W., Kimmel, S. R., Ullmann, B. and Schilling, T. F. (1995). Stages of embryonic development of the zebrafish. *Dev. Dyn.* **203**, 253-310.
Kintner, C. R. and Brockes, J. P. (1984). Monoclonal antibodies identify blastemal cells derived from dedifferentiating limb regeneration. *Nature* **308**, 67-69.
Lenhoff, H. M. and Lenhoff, S. G. (1991). Abraham Trembley and the origins of research on regeneration in animals. In *A History of Regeneration Research: Milestones in the Evolution of a Science* (ed. C. E. Dinsmore), pp. 47-66. Cambridge: Cambridge University Press.
Lister, J. A., Robertson, C. P., Lepage, T., Johnson, S. L. and Raible, D. W. (1999). nacre encodes a zebrafish microphthalmia-related protein that regulates neural-crest-derived pigment cell fate. *Development* **126**, 3757-3767.
Mackenzie, M. A., Jordan, S. A., Budd, P. S. and Jackson, I. J. (1997). Activation of the receptor tyrosine kinase Kit is required for the proliferation of melanoblasts in the mouse embryo. *Dev. Biol.* **192**, 99-107.
Medico, E., Gambarotta, G., Gentile, A., Comoglio, P. M. and Soriano, P. (2001). A gene trap vector system for identifying transcriptionally responsive genes. *Nat. Biotechnol.* **19**, 579-582.
Michalopoulos, G. K. and DeFrances, M. C. (1997). Liver regeneration. *Science* **276**, 60-66.
Milos, N. and Dingle, A. D. (1978). Dynamics of pigment pattern formation in the zebrafish, Brachydanio rerio. I. Establishment and regulation of the lateral line melanophore stripe during the first eight days of development. *J. Exp. Zool.* **205**, 205-216.
Morgan, T. H. (1901). *Regeneration*. New York: The Macmillan Co.
Moridani, M. Y., Cheon, S. S., Khan, S. and O'Brien, P. J. (2002). Metabolic activation of 4-hydroxyanisole by isolated rat hepatocytes. *Drug Metab. Dispos.* **30**, 1063-1069.
Morrison, S. J., Uchida, N. and Weissman, I. L. (1995). The biology of hematopoietic stem cells. *Annu. Rev. Cell Dev. Biol.* **11**, 35-71.
Naish, S., Cooksey, C. J. and Riley, P. A. (1988). Initial mushroom tyrosinase-catalysed oxidation product of 4-hydroxyanisole is 4-methoxy-ortho-benzoquinone. *Pigment Cell Res.* **1**, 379-381.
Nishimura, E. K., Jordan, S. A., Oshima, H., Yoshida, H., Osawa, M., Moriyama, M., Jackson, I. J., Barrandon,Y., Miyachi, Y. and Nishikawa, S. (2002). Dominant role of the niche in melanocyte stem-cell fate determination. *Nature* **416**, 854-860.
Page-McCaw, P. S., Chung, S. C., Muto, A., Roeser, T., Staub, W., Finger-Baier, K. C., Korenbrot, J. I. and Baier, H. (2004). Retinal network adaptation to bright light requires tyrosinase. *Nat. Neurosci.* **7**, 1329-1336.
Parichy, D. M. (2003). Pigment patterns: fish in stripes and spots. *Curr. Biol.* **13**, R947-R950.
Parichy, D. M., Rawls, J. F., Pratt, S. J., Whitfield, T. T. and Johnson, S. L. (1999). Zebrafish sparse corresponds to an orthologue of c-kit and is required for the morphogenesis of a subpopulation of melanocytes, but is not essential for hematopoiesis or primordial germ cell development. *Development* **126**, 3425-3436.
Parichy, D. M., Ransom, D. G., Paw, B., Zon, L. I. and Johnson, S. L. (2000). An orthologue of kit-related gene fms is required for development of neural crest-derived xanthophores and a subpopulation of adult melanocytes in the zebrafish, Danio rerio. *Development* **127**, 3031-3044.
Parichy, D. M., Turner, J. M. and Parker, N. B. (2003). Essential role for puma in development of postembryonic neural crest-derived cell lineages in zebrafish. *Dev. Biol.* **256**, 221-241.
Park, H. D., Ortmeyer, A. B. and Blankenbaker, D. P. (1970). Cell division during regeneration in Hydra. *Nature* **227**, 617-619.
Patton, E. E., Widlund, H. R., Kutok, J. L., Kopani, K. R., Amatruda, J. F., Murphey, R. D., Berghmans, S., Mayhall, E. A., Traver, D., Fletcher, C. D. et al. (2005). BRAF mutations are sufficient to promote nevi formation and cooperate with p53 in the genesis of melanoma. *Curr. Biol.* **15**, 249-254.
Peterson, R. T., Link, B. A., Dowling, J. E. and Schreiber, S. L. (2000). Small molecule developmental screens reveal the logic and timing of vertebrate development. *Proc. Natl. Acad. Sci. USA* **97**, 12965-12969.
Poleo, G., Brown, C. W., Laforest, L. and Akimenko, M. A. (2001). Cell proliferation and movement during early fin regeneration in zebrafish. *Dev. Dyn.* **221**, 380-390.
Potten, C. S. and Loeffler, M. (1990). Stem cells: attributes, cycles, spirals, pitfalls and uncertainties. Lessons for and from the crypt. *Development* **110**, 1001-1020.
Raible, D. W., Wood, A., Hodsdon, W., Henion, P. D., Weston, J. A. and Eisen, J. S. (1992). Segregation and early dispersal of neural crest cells in the embryonic zebrafish. *Dev. Dyn.* **195**, 29-42.
Rawls, J. F. and Johnson, S. L. (2000). Zebrafish kit mutation reveals primary and secondary regulation of melanocyte development during fin stripe regeneration. *Development* **127**, 3715-3724.
Rawls, J. F. and Johnson, S. L. (2001). Requirements for the kit receptor tyrosine kinase during regeneration of zebrafish fin melanocytes. *Development* **128**, 1943-1949.
Rawls, J. F. and Johnson, S. L. (2003). Temporal and molecular separation of the kit receptor tyrosine kinase's roles in zebrafish melanocyte migration and survival. *Dev. Biol.* **262**, 152-161.
Rawls, J. F., Mellgren, E. M. and Johnson, S. L. (2001). How the zebrafish gets its stripes. *Dev. Biol.* **240**, 301-314.
Rawls, J. F., Samuel, B. S. and Gordon, J. I. (2004). Gnotobiotic zebrafish reveal evolutionarily conserved responses to the gut microbiota. *Proc. Natl. Acad. Sci. USA* **101**, 4596-4601.
Riley, P. A. (1985). Radicals and melanomas. *Philos. Trans. R. Soc. Lond. B Biol. Sci.* **311**, 679-689.
Riley, P. A., Sawyer, B. and Wolf, M. A. (1975). The melanocytotoxic action of 4-hydroxyanisole. *J. Invest. Dermatol.* **64**, 86-89.
Rustin, G. J., Stratford, M. R., Lamont, A., Bleehen, N., Philip, P. A., Howells, N., Watfa, R. R. and Slack, J. A. (1992). Phase I study of intravenous 4-hydroxyanisole. *Eur. J. Cancer* **28A**, 1362-1364.

Siminovitch, L., McCulloch, E. A. and Till, J. E. (1963). The distribution of colony-forming cells among spleen colonies. *J. Cell Physiol.* **62**, 327-336.
Spangrude, G. J., Heimfeld, S. and Weissman, I. L. (1988). Purification and characterization of mouse hematopoietic stem cells. *Science* **241**, 58-62.
Sugimoto, M., Uchida, N. and Hatayama, M. (2000). Apoptosis in skin pigment cells of the medaka, Oryzias latipes (Teleostei), during long-term chromatic adaptation: the role of sympathetic innervation. *Cell Tissue Res.* **301**, 205-216.
Thibaudeau, G. and Holder, S. (1998). Cellular plasticity among axolotl neural crest-derived pigment cell lineages. *Pigment Cell Res.* **11**, 38-44.
Weinstein, G. D. and Frost, P. (1968). Abnormal cell proliferation in psoriasis. *J. Invest. Dermatol.* **50**, 254-259.
Westerfield, M. (1993). *The zebrafish book: A Guide for the Laboratory use of Zebrafish*. Eugene, OR: University of Oregan Press.
Wilkie, A. L., Jordan, S. A. and Jackson, I. J. (2002). Neural crest progenitors of the melanocyte lineage: coat colour patterns revisited. *Development* **129**, 3349-3357.
Yang, C. T., Sengelmann, R. D. and Johnson, S. L. (2004). Larval melanocyte regeneration following laser ablation in zebrafish. *J. Invest. Dermatol.* **123**, 924-929.